One-step Synthesis of a Cyclic 2,17-Dioxo[3,3](4,4')biphenylophane and First Preparation of a Microporous Polymer Network from a Macrocyclic Precursor by Cyclotrimerization

Suman Kalyan Samanta,[a]* Eduard Preis,[a] Christian W. Lehmann,[b] Richard Goddard,[b] Saientan Bag,[c] Prabal K. Maiti,[c] Gunther Brunklaus[d] and Ullrich Scherf[a]

[a] *Macromolecular Chemistry Group and Institute for Polymer Technology, Wuppertal University, Gauss-Strasse 20, 42119 Wuppertal, Germany. E-mail: sksiisc@gmail.com, scherf@uni-wuppertal.de*

[b] *Max-Planck-Institut für Kohlenforschung, Kaiser-Wilhelm-Platz 1, 45470 Mülheim an der Ruhr, Germany.*

[c] *Center for Condensed Matter Theory, Department of Physics, Indian Institute of Science, Bangalore 560 012, India.*

[d] *Westfälische Wilhelms-Universität, Institut für Physikalische Chemie, Corrensstr. 28/30, 48149 Münster, Germany.*

Electronic Supplementary Information (ESI)

Experimental Section:

Materials and Methods: All reagents, starting materials, and silica gel for TLC and column chromatography were obtained from the best known commercial sources and were used without further purification, as appropriate. Solvents were distilled and dried prior to use. Reactions were carried out under argon atmosphere with the use of standard and Schlenk techniques. Solution phase ^{1}H and ^{13}C NMR data of the macrocycle was recorded on a Bruker ARX 400-spectrometer. Chemical shifts were reported in ppm downfield from the internal standard, tetramethylsilane. FT-IR spectra were recorded on a JASCO FT/IR-4200 spectrometer and were reported in wavenumbers (cm^{-1}). The thermogravimetric analysis were performed on a Mettler 1 STAR^{e} system (Mettler–Toledo) with a heating rate of 10 ^{o}C/min. UV-vis and fluorescence spectra were recorded in a JASCO V-670 spectrophotometer and HORIBA FluoroMax-4 spectrofluorometer respectively.

Solid-State NMR measurements: Solid-state ^{13}C CPMAS spectra were recorded at 100.67 MHz using a Bruker Avance I 400 spectrometer with a contact time of 2.5 ms averaging 65536 scans at a repetition delay of 1s. All experiments were carried out at room temperature with a standard Bruker 4 mm double resonance MAS probe spinning at 12.5 kHz, typical $\pi/2$-pulse lengths of 3 μs and SPINAL64 proton decoupling (rf-field strength of 83.3 kHz). The

spectra were referenced with respect to tetramethyl silane (TMS) using solid adamantane as secondary standard (29.46 ppm for ^{13}C).

Nitrogen sorption measurements. The nitrogen sorption measurements were carried out on a BELSORB Max (Bel Japan Inc.) instrument. The surface areas were estimated using the BET model in the pressure range p/p_o from 0.05 – 0.25. The total pore volume was calculated at a relative pressure of 0.95.

Treatment (washing) with supercritical carbon dioxide. All samples were soaked with absolute ethanol for 72 h prior to the supercritical drying process. The drying procedure was carried out in a supercritical point dryer from TousimisTM (Samdri – 795) with liquid CO_2 (Messer) as carbon dioxide source. The dry samples were obtained after consecutive four drying cycles: The ethanol-containing samples were placed inside the dryer and the ethanol was replaced by rinsing with liquid CO_2(l) over a period of 15 min. Then the chamber was sealed and the temperature was raised to 40 °C resulting in a chamber pressure of around 1300 psi which is well above the critical point of CO_2. The chamber was held in this condition above the critical point for 1 h. This procedure was repeated successively for another three times with the following modifications: second run: 5 min purging, 1 h supercritical conditions, third run: 5 min purging, 2.5 h supercritical conditions; and the last run 5 min purging, 14 h supercritical conditions.

Theoretical calculations. The conformal search was carried out using the random rotor search method using Avogadro 1.1.1[1]. The conformers generated were geometry optimized using MMFF94 force field and steepest descent algorithm as implemented in Avogadro 1.1.1[1]. After geometry optimization the energy of the conformers were noted and the distinct conformers within energy 20 kJ/mol from the lowest energy conformer were chosen for further calculation.

The chosen conformers were further geometry optimized using Gaussian 09[2] at M06-2X/6-31G(d) level of theory. The polarisable continuum model (PCM) with static dielectric constant 78.355 and dynamic dielectric constant 1.777 were used to model the effect of surrounding solvent. Geometries obtained at this stage was reported as the geometries of the conformer and further used to calculate energies of the conformers.

The final energies of the conformers were calculated as sum of the potential energies (single point energy) and zero point vibrational energies. Both single point energy and zero point vibrational energy were calculated using Gaussian 09[2] at the M06-2X/6-31G(d) and the M06-1/6-31G(d) level of theory.[3] The PCM model with same parameters as used in geometry optimization was used in this case. We have also calculated the relative energy of the conformers with respect to lowest energy conformer.

Synthesis:

Synthesis of the macrocycle MC (2,17-dioxo[3,3](4,4')biphenylophane): Synthesis of 2,17-dioxo[3,3](4,4')biphenylophane was accomplished in one-step from 1,3-bis(4-bromophenyl)propan-2-one in a Yamamoto coupling procedure. First, 1,3-bis(4-

bromophenyl)propan-2-one was prepared from 2-(4-bromophenyl)acetic acid following a literature procedure.[4] In a 250 mL dry schlenk flask, bis(1,5-cyclooctadiene)nickel(0) [$Ni(COD)_2$] (0.560 g, 2.038 mmol) and 2,2'-bipyridine (0.318 g, 2.038 mmol) were added in a glovebox. The flask was then taken out from the glovebox and 1,5-cyclooctadiene (0.250 ml, 2.038 mmol) and 15 mL of dry DMF were injected under argon atmosphere. The mixture was stirred at 70 ^oC in the dark for about 30 min to generate the deep blue catalyst solution. An oven dried dropping funnel filled with 0.5 g (1.358 mmol) 1,3-bis(4-bromophenyl)propan-2-one dissolved in 60 mL of DMF was carefully attached to the catalyst-containing Schlenk flask flushed thoroughly with argon. The monomer was added dropwise in such a rate that the addition was completed in about 3-4 h. The mixture was then stirred at 70 ^oC in the dark for 2 days under argon atmosphere. Then it was cooled to RT and acidified with 2N HCl. The product was extracted with DCM, washed with water, saturated $NaHCO_3$ solution, aqueous NaEDTA solution, and finally with brine solution. The organic layer was dried over magnesium sulphate, all solvents removed by rotary evaporation. Silica gel column chromatography (eluted with 4:1 ethylacetate/hexane) yielded 2,17-dioxo[3,3](4,4')biphenylophane as white, crystalline solid (0.085 g, yield 30%). IR ($\bar{\upsilon}$, cm^{-1}): 1690 (C=O); ^1H NMR (400 MHz, $CDCl_3$) δ 6.98 (d, J = 8.3 Hz, 8H), 6.92 (d, J = 8.3 Hz, 8H), 3.79 (s, 8H); ^{13}C NMR (100 MHz, $CDCl_3$) δ 206.40, 139.15, 133.17, 129.55, 126.81, 51.50; FD-MS: calculated for $C_{30}H_{24}O_2$: 416.5, found 416.8.

Synthesis of the porous materials using MSA: Synthesis of the polymer networks was carried out as reported in our previous report[5] using an acid-catalysed cyclotrimerization protocol. To a 100 mL flask 70 mg (0.168 mmol) of 2,17-dioxo[3,3](4,4')biphenylophane (macrocycle **MC**) and 4 mL of ODCB were added. Next, 0.7 mL of methanesulfonic acid (MSA) were injected. The mixture was heated up to 180°C for 24 h under argon atmosphere. After cooling down to room temperature the mixture was poured into cold water and isolated by filtration. The dark colored product was purified by Soxhlet extraction with water, acetone and chloroform (24 h each). The product was dried with supercritical carbon dioxide to give 55 mg (85 %) of a dark colored solid.

Synthesis of the porous materials using $TiCl_4$: Titanium tetrachloride (237 mg, 1.248 mmol) and 5 mL of 1,2-dichlorobenzene (ODCB) were placed in to a 100 mL flask and heated to reflux. To this mixture, the macrocycle **MC** (40 mg, 0.096 mmol) dissolved in 5 mL ODCB was injected and the mixture was refluxed for 72 h under argon. After cooling down to room temperature the reaction mixture was poured into ice/conc. aqueous hydrochloric acid and stirred for 48 h. The precipitate was isolated by filtration, neutralized with 5 M aqueous sodium hydroxide solution and extracted with water, acetone and chloroform in a Soxhlet apparatus. After drying with supercritical carbon dioxide, the product was isolated as dark colored solid (44 mg, 110%). The yield of >100% indicates for the presence of non-reacted $-CH_2-CO-$ end groups and/or titanium oxide impurities.

Supporting Figures

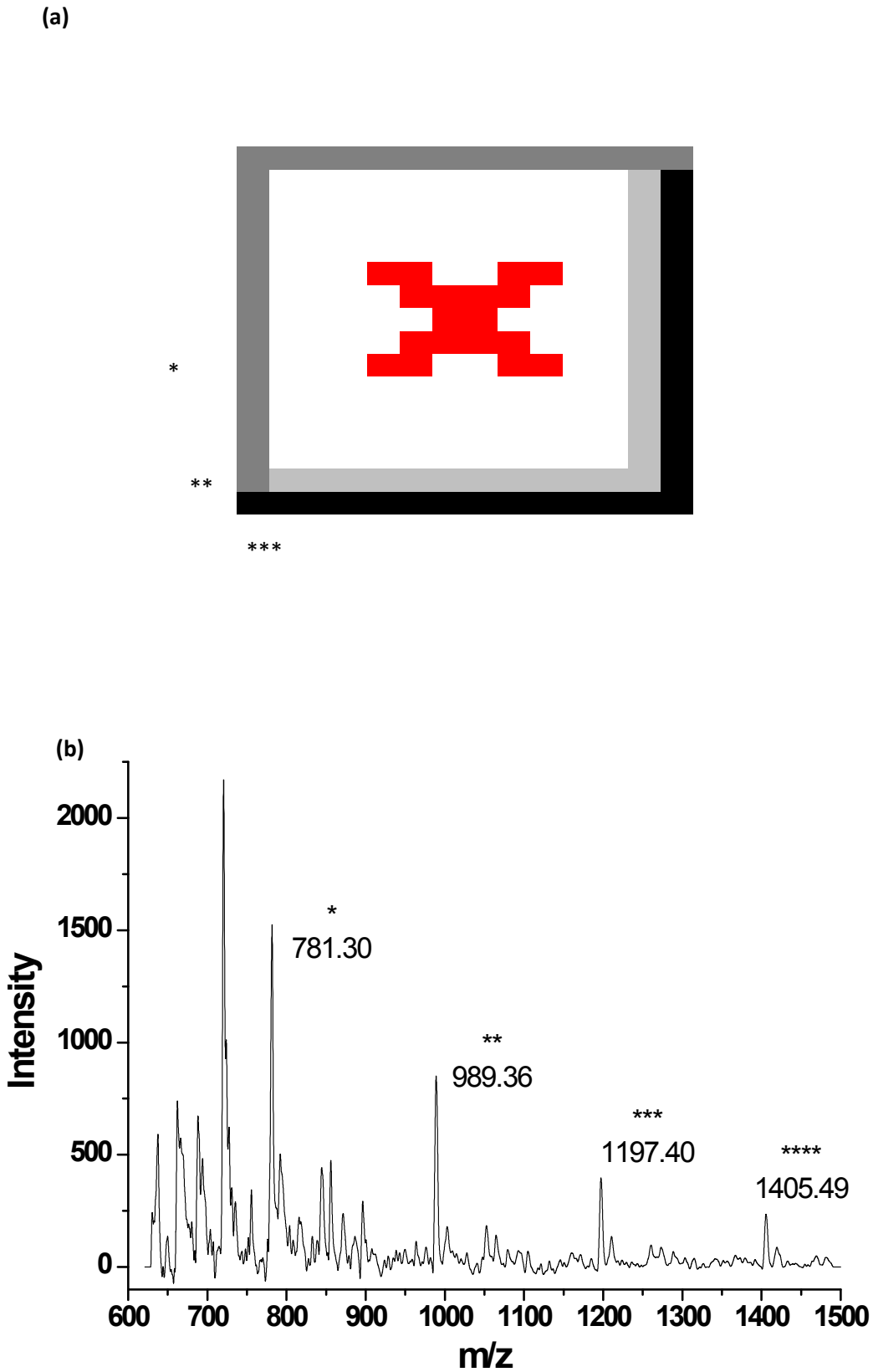

Figure S1. MALDI-TOF mass spectrometry of the linear acyclic by-products during Yamamoto coupling (a) the full spectrum and (b) baseline-corrected spectrum (dibromo-terminated, linear trimer (*), tetramer (**), pentamer (***) *etc*).

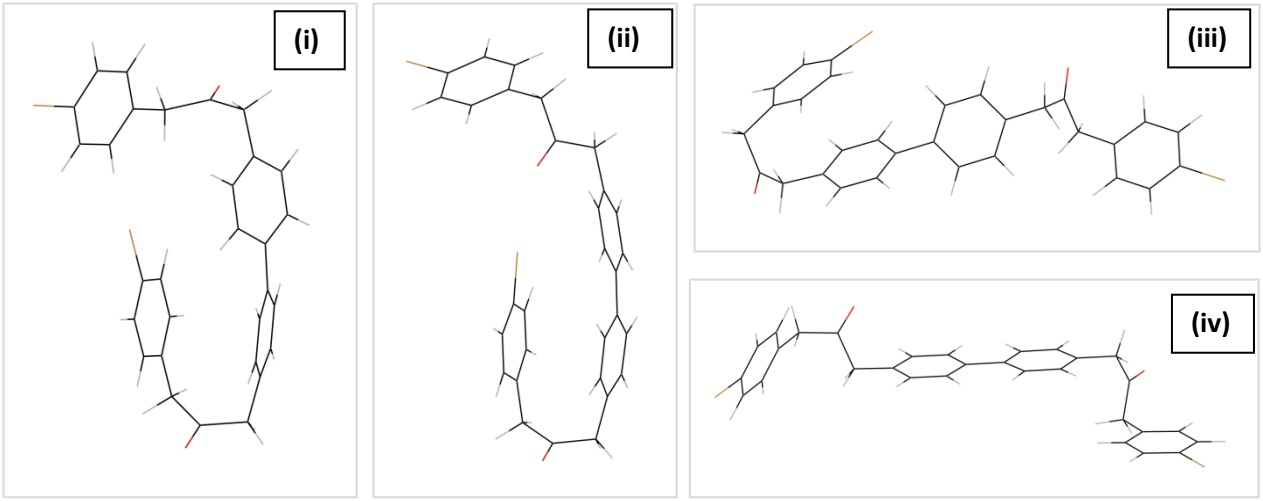

Figure S2. Calculated geometries of the linear, acyclic dimer: the folded conformations (**i**) and (**ii**) show lower total energies if compared to the linear, open chain conformations (**iii**) and (**iv**).

Table S1. Calculated total energies for geometries (**i**) to (**iv**) of the linear, acyclic dimers presented in Figure S2.

Conformation	Total Energy (M06-2X/6-31G(d), kcal/mol)	Relative Energy (M06-2X/6-31G(d), kcal/mol)	Total Energy (M06-1/6-31G(d), kcal/mol)	Relative Energy (M06-1/6-31G(d), kcal/mol)
(i)	-4047872.4539 ± 0.7	0	-4047796.7402 ± 0.9	0
(ii)	-4047871.5941 ± 0.7	0.8598	-4047795.2225 ± 0.9	1.5177
(iii)	-4047870.1328 ± 0.7	2.3211	-4047793.7760 ± 0.9	2.9642
(iv)	-4047865.5781 ± 0.7	6.6758	-4047789.5569 ± 0.9	7.1833

In our DFT calculations both levels that have been applied M06-2X/6-31G(d) or M06-1/6-31G(d) resulted in very similar relative energies of the conformers (with respect to lowest energy conformer). Thermal fluctuation at room temperature is in the order of K_bT (0.593 kcal/mol) which might lead to inter-conversion between the folded conformers (**i**) and (**ii**). However, the energy difference between the folded (**i**) and the linear conformer (**iv**) is ~6-**7** kcal/mol which is close to ~12 K_bT. Therefore, it is very unlikely that thermal fluctuations cause inter-conversions between folded and linear conformers.

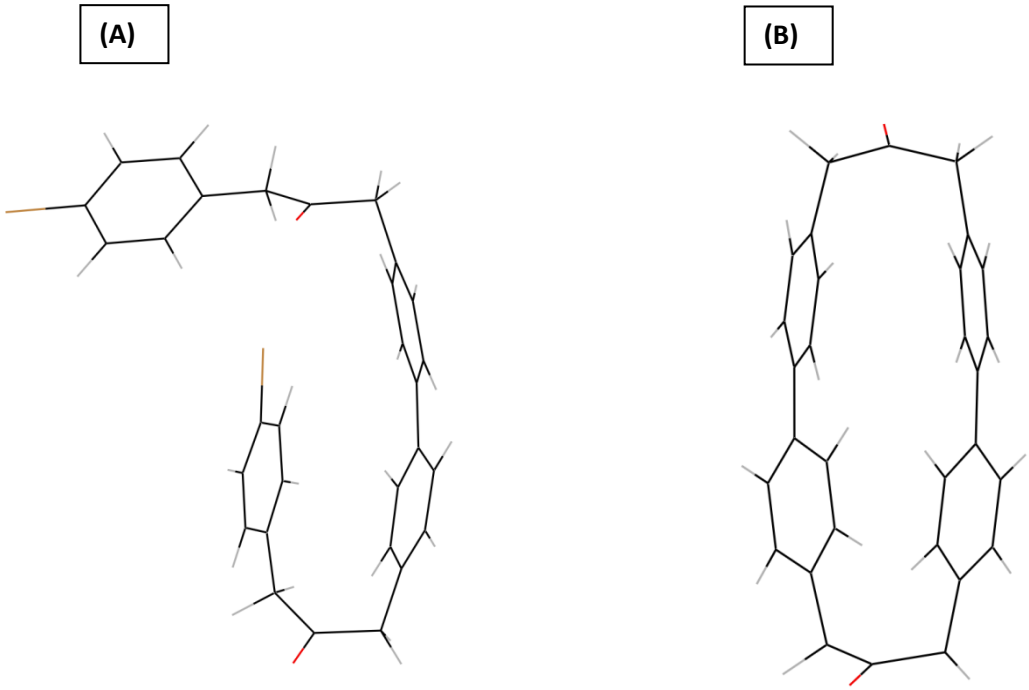

Figure S3. (A) Optimized transition state geometry for the formation of macrocycle and (B) optimized geometry of the macrocycle. Although, the crystal structure shows an *anti*-orientation of the two carbonyl moieties, theoretical calculations predict similar energies for both *anti*- or *syn*-oriented carbonyl groups.

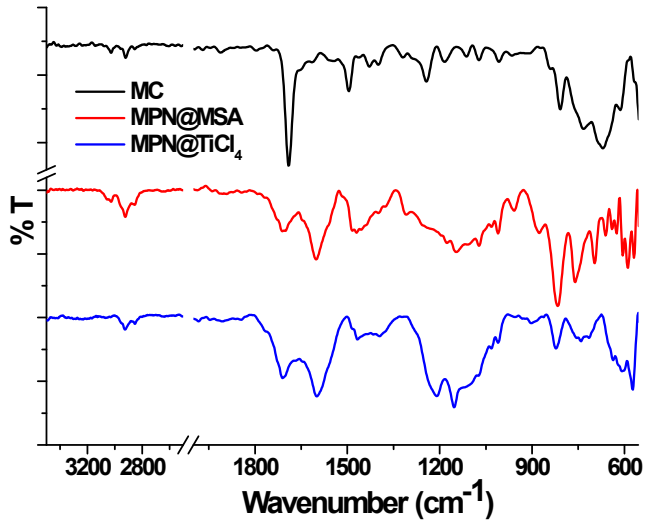

Figure S4. Comparison in the FT-IR spectra of the microporous polymer networks and the macrocyclic precursor **MC**.

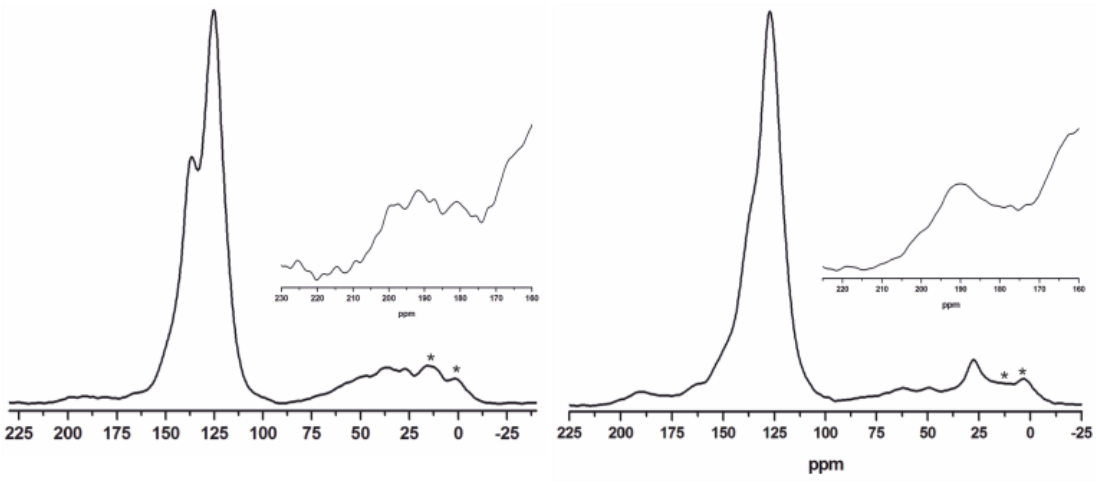

Figure S5. $^{13}C\{^{1}H\}$ CPMAS NMR spectra of MPNs made with MSA (left) and $TiCl_4$ (right), recorded at 100.67 MHz and 12.5 kHz MAS. 65536 scans were averaged at a contact time of 2.5 ms and repetition delay of 1s. Note that the radiofrequency field strengths for ^{1}H and ^{13}C were set to 83.3 kHz; occurring spinning sidebands are marked with asterisks. A zoom of the ^{13}C chemical shift region attributed to keto groups is displayed in the inserts.

The ^{13}C CPMAS NMR spectra of both MPNs reveal noticeable differences in the chemical shift region attributable to keto-moieties (170 – 210 ppm) and CH_2-units (25 – 60 ppm), thus reflecting structural differences of the MPNs made with MSA or $TiCl_4$. While an unambiguous peak assignment is not feasible based on the current data, it is clearly seen that in case of MPNs made with MSA at least three peaks centred at 180, 190 and 198.8 ppm could be resolved (at comparable signal intensities) while the signal around 190 ppm is more pronounced for MPNs prepared with $TiCl_4$.

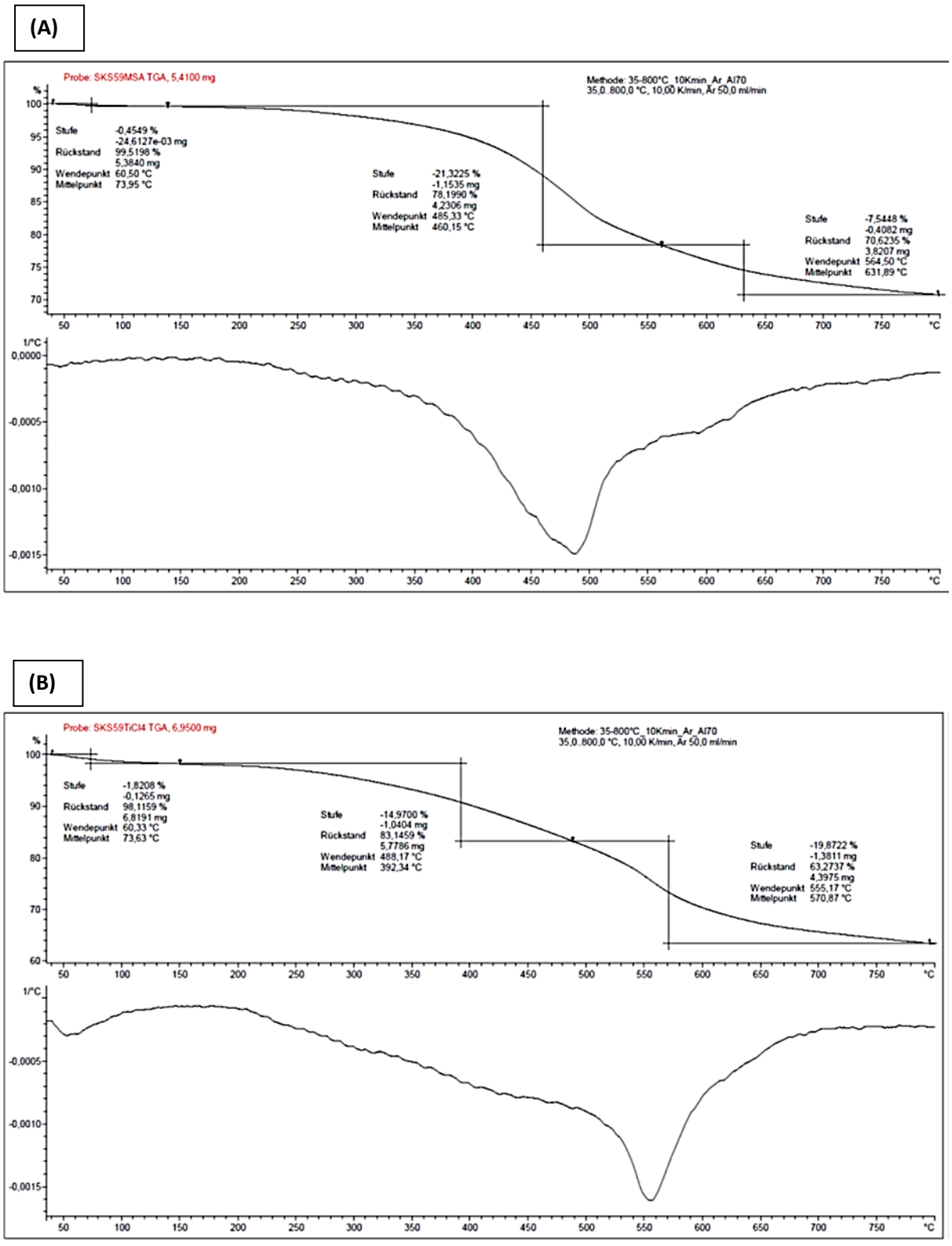

Figure S6. Thermogravimetric analyses of the porous polymer networks prepared using (A) MSA and (B) $TiCl_4$ in argon.

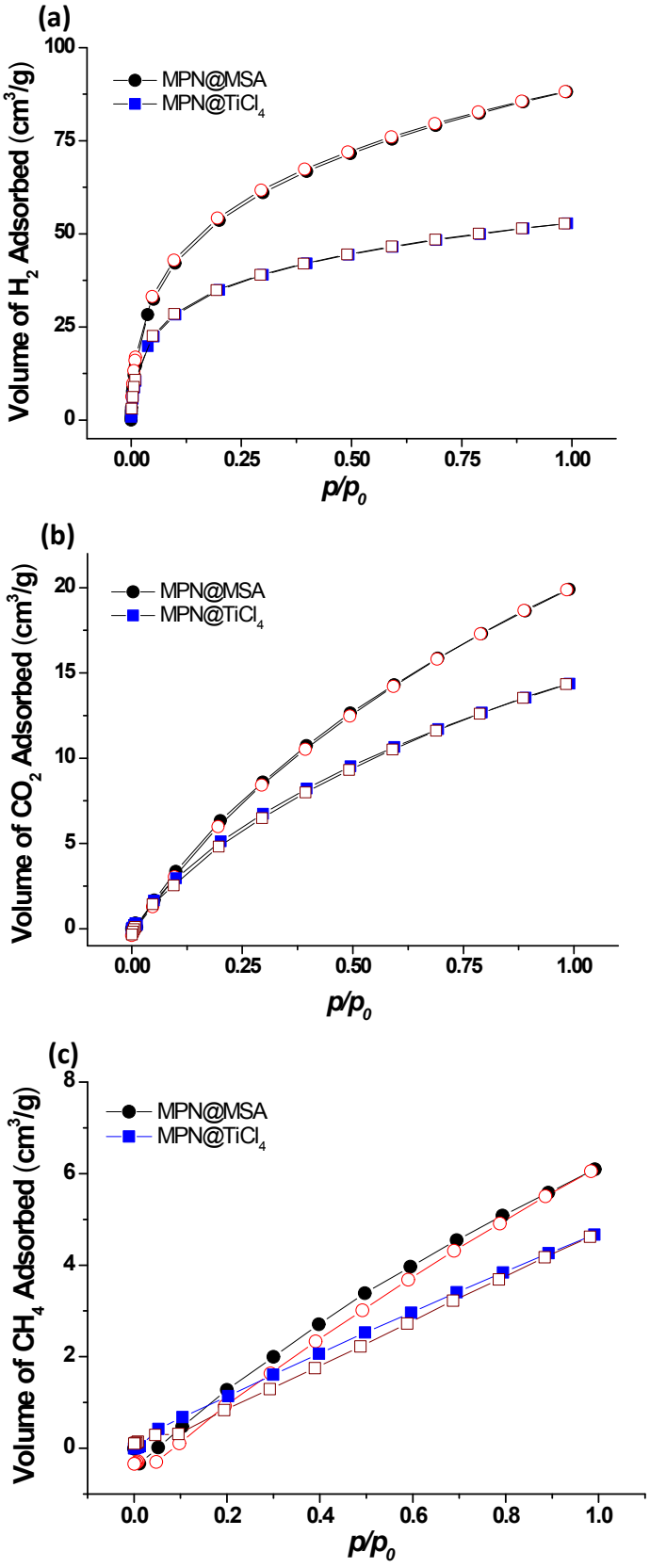

Figure S7. Sorption isotherms for the microporous polymer networks MPN@MSA and MPN@$TiCl_4$ for (a) H_2, (b) CO_2 and (c) CH_4 gas (filled symbols represent adsorption and empty symbols represent desorption branches).

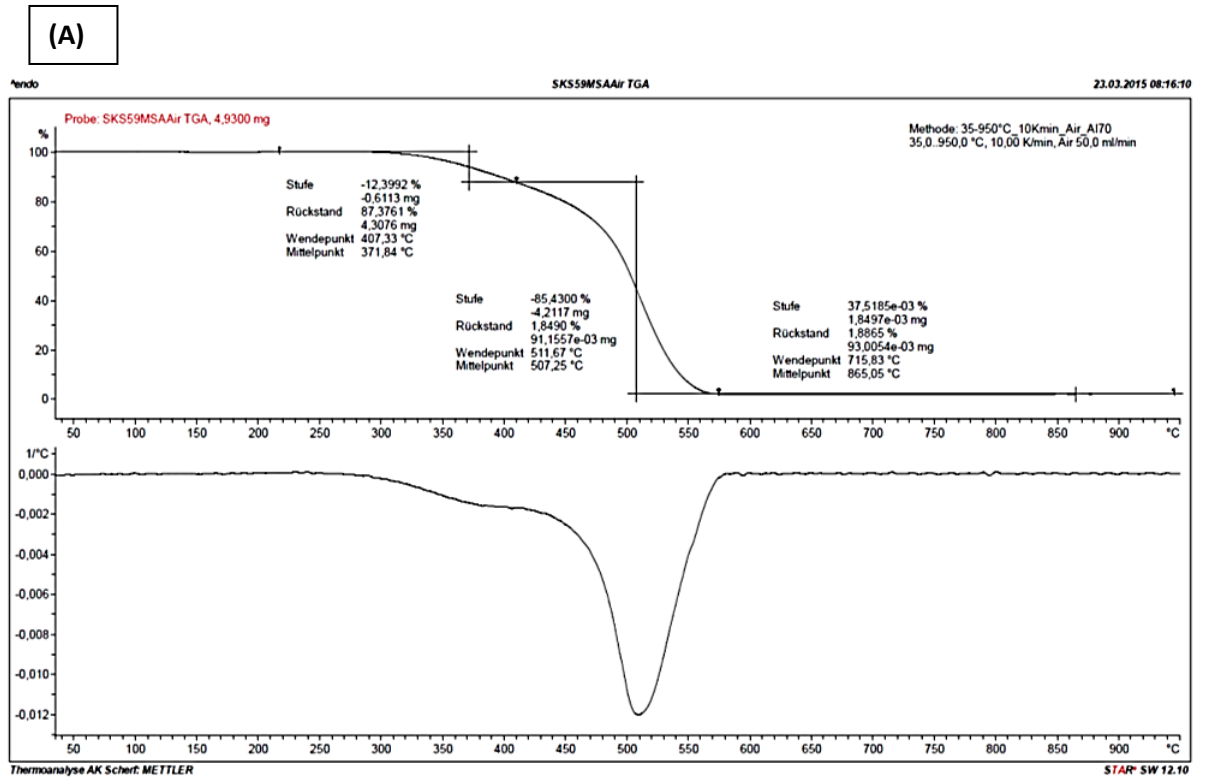

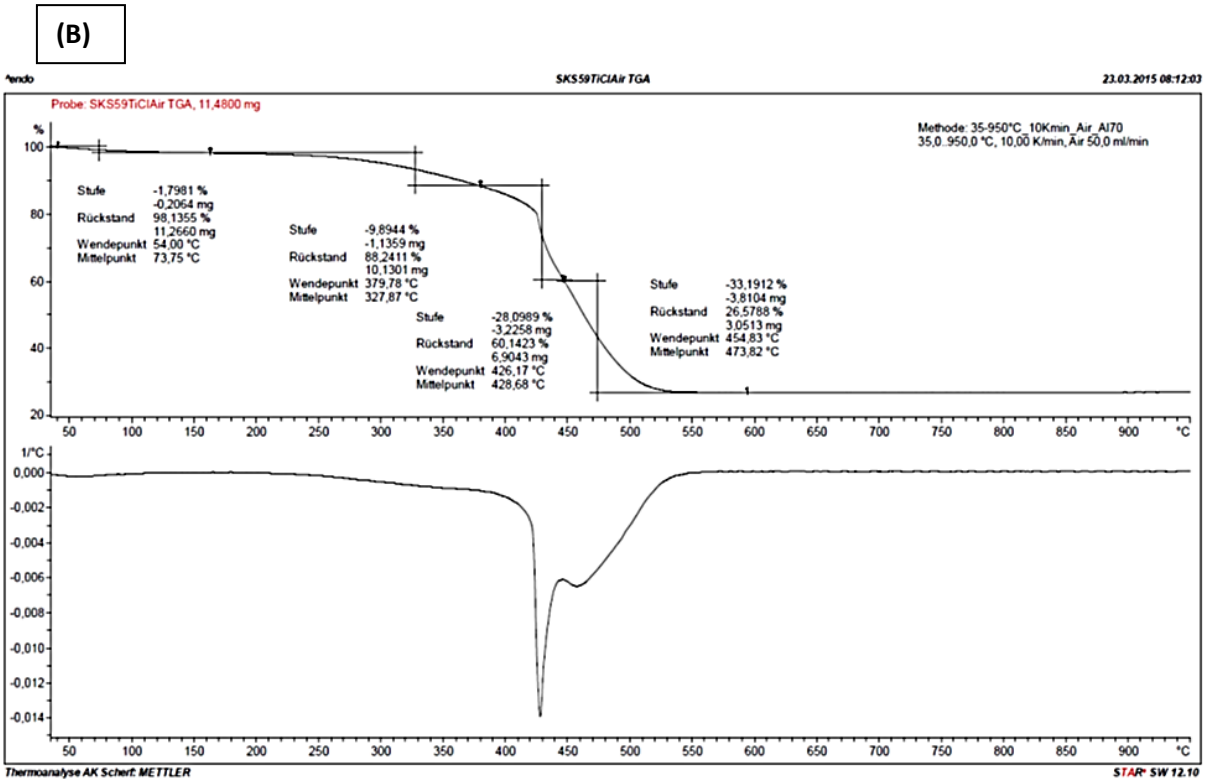

Figure S8. Thermogravimetric analyses of the porous polymer networks prepared with (A) MSA and (B) $TiCl_4$ in air, the residue at 950 °C was *ca.* 1.9% for MPN@MSA and 26.6% for MPN@$TiCl_4$.

References:

[1] Avogadro: an open-source molecular builder and visualization tool. Version 1.1.1. http://avogadro.openmolecules.net/.

[2] Gaussian 09, Revision **D.01**, M. J. Frisch, G. W. Trucks, H. B. Schlegel, G. E. Scuseria, M. A. Robb, J. R. Cheeseman, G. Scalmani, V. Barone, B. Mennucci, G. A. Petersson, H. Nakatsuji, M. Caricato, X. Li, H. P. Hratchian, A. F. Izmaylov, J. Bloino, G. Zheng, J. L. Sonnenberg, M. Hada, M. Ehara, K. Toyota, R. Fukuda, J. Hasegawa, M. Ishida, T. Nakajima, Y. Honda, O. Kitao, H. Nakai, T. Vreven, J. A. Montgomery, Jr., J. E. Peralta, F. Ogliaro, M. Bearpark, J. J. Heyd, E. Brothers, K. N. Kudin, V. N. Staroverov, R. Kobayashi, J. Normand, K. Raghavachari, A. Rendell, J. C. Burant, S. S. Iyengar, J. Tomasi, M. Cossi, N. Rega, J. M. Millam, M. Klene, J. E. Knox, J. B. Cross, V. Bakken, C. Adamo, J. Jaramillo, R. Gomperts, R. E. Stratmann, O. Yazyev, A. J. Austin, R. Cammi, C. Pomelli, J. W. Ochterski, R. L. Martin, K. Morokuma, V. G. Zakrzewski, G. A. Voth, P. Salvador, J. J. Dannenberg, S. Dapprich, A. D. Daniels, Ö. Farkas, J. B. Foresman, J. V. Ortiz, J. Cioslowski, and D. J. Fox, Gaussian, Inc., Wallingford CT, 2009.

[3] C. Storz, M. Badoux, C. M. Hauke, T. Šolomek, A. Kühnle, T. Bally and A. F. M. Kilbinger, *J. Am. Chem. Soc.*, 2014, **136**, 12832-12835.

[4] N. Venkatramaiah, S. Kumar, S. Patil, *Chem. Eur. J.,* 2012, **18**, 14745 – 14751.

[5] R. S. Sprick, A. Thomas and U. Scherf, *Polym. Chem.*, 2010, **1**, 283-285.

Single crystal X-ray structure analysis of MC

Table S2. Crystal data and structure refinement.

Identification code	**MC**	
Empirical formula	$C_{30}H_{24}O_2$	
Color	colourless	
Formula weight	416.49 $g \cdot mol^{-1}$	
Temperature	150 K	
Wavelength	0.8 Å	
Crystal system	monoclinic	
Space group	C 2/c, (no. 15)	
Unit cell dimensions	a = 31.067(15) Å	α= 90°.
	b = 13.835(6) Å	β= 93.254(11)°.
	c = 15.670(7) Å	γ = 90°.
Volume	6724(5) $Å^3$	
Z	12	
Density (calculated)	1.234 $Mg \cdot m^{-3}$	
Absorption coefficient	0.097 mm^{-1}	
F(000)	2640 e	
Crystal size	0.440 x 0.016 x 0.010 mm^3	
θ range for data collection	1.478 to 32.051°.	
Index ranges	$-40 \le h \le 41$, $-17 \le k \le 17$, $-20 \le l \le 20$	
Reflections collected	72812	
Reflections with I>2σ(I)	43956	
Completeness to θ = 28.685°	97.8 %	
Absorption correction	Semi-empirical from equivalents	
Max. and min. transmission	1.0 and 0.452782	
Refinement method	Full-matrix least-squares on F^2	
Data / restraints / parameters	72812 / 0 / 434	
Goodness-of-fit on F^2	1.049	
Final R indices [I>2σ(I)]	R_1 = 0.0858	wR^2 = 0.1739
R indices (all data)	R_1 = 0.1448	wR^2 = 0.1979
Extinction coefficient	0	
Largest diff. peak and hole	0.448 and -0.446 $e \cdot Å^{-3}$	
Twin law	[1.0 0.0 0.216 0.0 -1.0 0.0 0.0 0.0 -1.0]	
Batch scale factor for minor component	0.2374(12)	

Table S3. Atomic coordinates and equivalent isotropic displacement parameters (Å^2). U_{eq} is defined as one third of the trace of the orthogonalized U_{ij} tensor.

	x	y	z	U_{eq}
C(1)	0.4530(1)	-0.0001(3)	0.2887(2)	0.024(1)
C(2)	0.4554(1)	0.1045(3)	0.3236(2)	0.027(1)
O(2)	0.2263(1)	-0.0552(2)	0.8641(2)	0.046(1)
C(3)	0.4202(1)	0.1223(2)	0.3882(2)	0.024(1)
O(3)	0.3852(1)	0.5243(2)	0.4049(2)	0.049(1)
C(4)	0.4307(1)	0.1425(2)	0.4751(2)	0.024(1)
C(5)	0.3983(1)	0.1448(2)	0.5354(2)	0.023(1)
C(6)	0.3542(1)	0.1287(2)	0.5102(2)	0.021(1)
C(7)	0.3437(1)	0.1134(3)	0.4216(2)	0.027(1)
C(8)	0.3761(1)	0.1103(3)	0.3620(2)	0.027(1)
C(9)	0.3194(1)	0.1204(2)	0.5741(2)	0.022(1)
C(10)	0.3287(1)	0.0817(2)	0.6572(2)	0.024(1)
C(11)	0.2955(1)	0.0641(2)	0.7132(2)	0.026(1)
C(12)	0.2518(1)	0.0830(3)	0.6888(2)	0.025(1)
C(13)	0.2425(1)	0.1257(3)	0.6081(2)	0.028(1)
C(14)	0.2757(1)	0.1440(2)	0.5516(2)	0.026(1)
C(15)	0.2145(1)	0.0568(3)	0.7466(2)	0.032(1)
C(16)	0.2172(1)	-0.0453(3)	0.7869(2)	0.027(1)
C(17)	0.2074(1)	-0.1342(3)	0.7295(2)	0.032(1)
C(18)	0.2439(1)	-0.1516(3)	0.6679(2)	0.026(1)
C(19)	0.2395(1)	-0.1219(3)	0.5817(2)	0.030(1)
C(20)	0.2747(1)	-0.1260(3)	0.5283(2)	0.028(1)
C(21)	0.3156(1)	-0.1598(2)	0.5598(2)	0.021(1)
C(22)	0.3194(1)	-0.1943(2)	0.6453(2)	0.025(1)
C(23)	0.2842(1)	-0.1899(3)	0.6984(2)	0.028(1)
C(24)	0.3547(1)	-0.1510(2)	0.5064(2)	0.021(1)
C(29)	0.3945(1)	-0.1183(2)	0.5444(2)	0.025(1)
C(25)	0.3523(1)	-0.1685(2)	0.4167(2)	0.024(1)
C(28)	0.4300(1)	-0.0997(2)	0.4944(2)	0.025(1)
C(26)	0.3881(1)	-0.1507(3)	0.3673(2)	0.025(1)
C(27)	0.4274(1)	-0.1137(2)	0.4049(2)	0.023(1)
C(30)	0.4652(1)	-0.0848(3)	0.3498(2)	0.028(1)
C(31)	0.3780(1)	0.5063(3)	0.4802(2)	0.028(1)

C(32)	0.3676(1)	0.5885(3)	0.5427(2)	0.030(1)
C(33)	0.4059(1)	0.6142(3)	0.6056(2)	0.025(1)
C(34)	0.4443(1)	0.6556(2)	0.5763(2)	0.027(1)
C(35)	0.4808(1)	0.6706(2)	0.6326(2)	0.025(1)
C(36)	0.4798(1)	0.6458(2)	0.7208(2)	0.022(1)
C(37)	0.4405(1)	0.6103(3)	0.7504(2)	0.026(1)
C(38)	0.4043(1)	0.5944(3)	0.6936(2)	0.029(1)
C(39)	0.3786(1)	0.4011(3)	0.5133(2)	0.032(1)
C(40)	0.4150(1)	0.3833(2)	0.5829(2)	0.025(1)
C(41)	0.4585(1)	0.4022(3)	0.5661(2)	0.027(1)
C(42)	0.4917(1)	0.3930(2)	0.6305(2)	0.026(1)
C(43)	0.4823(1)	0.3637(2)	0.7147(2)	0.023(1)
C(44)	0.4388(1)	0.3417(2)	0.7304(2)	0.027(1)
C(45)	0.4056(1)	0.3508(3)	0.6654(2)	0.027(1)
O(1)	0.4407(1)	-0.0160(2)	0.2136(2)	0.034(1)

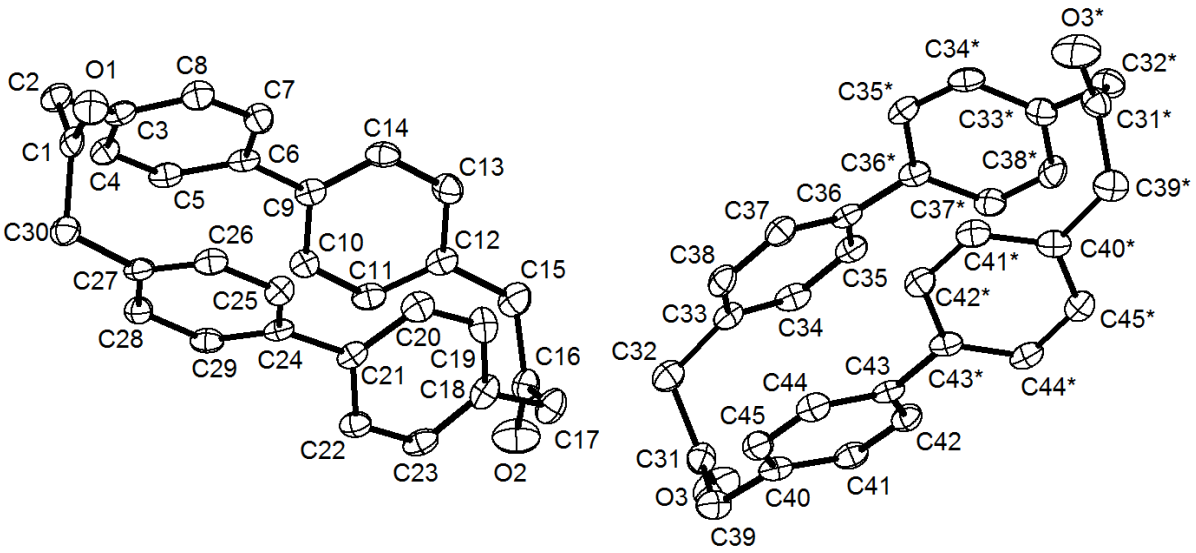

Figure S9. The molecular structure of **MC**

Data were collected on the SCD beamline at the ANKA Synchrotron Facility, Karlsruhe Institute of Technology, Karlsruhe Germany. The experimental apparatus was a Bruker D8 goniometer and and APEX II CCD detector. The crystal was cooled to 150 K using a Cryostream from Oxford Instruments. Data were integrated using the SAINT software of the APEX2 suite of computer programs (Bruker AXS). Data were absorption corrected by Gaussian integration and scaled using the program TWINABS (George Sheldrick, Bruker AXS).

The minimum and maximum estimated transmissions from the multi-scan scaling are 0.452782 and 1.0 (TWINABS). All crystals investigated were partially twinned. The crystal studied was twinned by rotation about a* [twin law: 1.0 0.0 0.216 0.0 -1.0 0.0 0.0 0.0 -1.0]. Refinement was carried out using data from the major domain. For the structure described here the refined occupancy of the second domain was 0.2374(12). The structure was refined using HKLF 5 data produced, using the program TWINABS for the major component.

Statistics of intensity data scaled with SADABS:

Resolution	#Data	#Theory	%Complete	Redundancy	Mean I	Mean I/s	Rmerge	Rsigma
Inf - 3.19	125	127	98.4	11.17	74.9	30.20	0.0590	0.0393
3.19 - 2.11	290	290	100.0	12.99	29.4	33.55	0.0543	0.0238
2.11 - 1.67	413	414	99.8	13.41	19.0	33.18	0.0541	0.0242
1.67 - 1.45	419	419	100.0	12.86	9.2	31.13	0.0590	0.0254
1.45 - 1.31	421	422	99.8	11.90	7.1	25.13	0.0703	0.0292
1.31 - 1.21	453	454	99.8	11.09	8.6	24.15	0.0695	0.0302
1.21 - 1.14	392	393	99.7	10.32	9.3	22.35	0.0676	0.0311
1.14 - 1.08	440	442	99.5	9.92	6.8	20.46	0.0768	0.0343
1.08 - 1.03	445	445	100.0	9.58	4.6	17.81	0.0923	0.0408
1.03 - 0.99	412	412	100.0	9.24	3.8	15.11	0.1045	0.0453
0.99 - 0.96	373	373	100.0	8.89	3.0	15.48	0.1209	0.0514
0.96 - 0.93	409	409	100.0	8.76	2.8	13.91	0.1300	0.0538
0.93 - 0.90	471	471	100.0	8.22	2.0	10.63	0.1603	0.0704
0.90 - 0.88	353	353	100.0	8.25	2.0	10.81	0.1735	0.0717
0.88 - 0.85	580	580	100.0	7.74	1.8	9.78	0.1997	0.0819
0.85 - 0.84	218	219	99.5	7.63	1.6	9.73	0.2106	0.0861
0.84 - 0.82	462	462	100.0	7.51	1.8	10.23	0.2134	0.0824
0.82 - 0.80	499	501	99.6	6.94	1.6	8.51	0.2525	0.0952
0.80 - 0.79	270	272	99.3	6.90	1.6	8.43	0.2710	0.0993
0.79 - 0.77	537	574	93.6	3.26	1.5	5.54	0.2984	0.1895
0.77 - 0.75	298	685	43.5	0.66	1.3	3.24	0.3088	0.3120
0.85 - 0.75	2284	2713	84.2	4.73	1.6	7.58	0.2441	0.1354
Inf - 0.75	8280	8717	95.0	8.45	6.7	16.54	0.0760	0.0405

Merged [A], lowest resolution = 15.64 Angstroms

99.9% of the diffraction data were complete to 0.82 \%A.

The absorption coeficient was calculated using the X-ray absorption coefficients corresponding to the wavelength of 0.8 \%A:

DISP $C 0.00473 0.00222 14.60850 !source kissel, Creaghb and Hubbell
DISP $H -0.00002 0.00000 0.66620 !source kissel, Creaghb and Hubbell
DISP $O 0.01495 0.00812 43.76101 !source kissel, Creaghb and Hubbell

Residual electron density in a difference Fourier synthesis after the final refinement cycles:

Highest peak 0.45 at 0.3311 0.9170 0.1655 [0.15 A from C10]
Deepest hole -0.45 at 0.1076 0.3635 0.0445 [1.38 A from C28]

Table S4. Bond lengths [Å] and angles [°].

C(1)-O(1)	1.236(4)	C(1)-C(30)	1.547(5)
C(1)-C(2)	1.547(5)	C(2)-C(3)	1.551(4)
C(2)-H(2A)	0.9900	C(2)-H(2B)	0.9900
O(2)-C(16)	1.235(4)	C(3)-C(4)	1.409(4)
C(3)-C(8)	1.420(4)	O(3)-C(31)	1.238(4)
C(4)-C(5)	1.419(5)	C(4)-H(4)	0.9500
C(5)-C(6)	1.422(4)	C(5)-H(5)	0.9500
C(6)-C(7)	1.423(4)	C(6)-C(9)	1.520(4)
C(7)-C(8)	1.413(5)	C(7)-H(7)	0.9500
C(8)-H(8)	0.9500	C(9)-C(14)	1.420(4)
C(9)-C(10)	1.423(5)	C(10)-C(11)	1.411(5)
C(10)-H(10)	0.9500	C(11)-C(12)	1.415(5)
C(11)-H(11)	0.9500	C(12)-C(13)	1.410(5)
C(12)-C(15)	1.552(5)	C(13)-C(14)	1.419(5)
C(13)-H(13)	0.9500	C(14)-H(14)	0.9500
C(15)-C(16)	1.547(5)	C(15)-H(15A)	0.9900
C(15)-H(15B)	0.9900	C(16)-C(17)	1.544(5)
C(17)-C(18)	1.550(5)	C(17)-H(17A)	0.9900
C(17)-H(17B)	0.9900	C(18)-C(19)	1.411(5)
C(18)-C(23)	1.418(5)	C(19)-C(20)	1.415(5)
C(19)-H(19)	0.9500	C(20)-C(21)	1.417(5)
C(20)-H(20)	0.9500	C(21)-C(22)	1.421(4)
C(21)-C(24)	1.518(4)	C(22)-C(23)	1.413(5)
C(22)-H(22)	0.9500	C(23)-H(23)	0.9500
C(24)-C(29)	1.417(4)	C(24)-C(25)	1.424(4)
C(29)-C(28)	1.413(5)	C(29)-H(29)	0.9500
C(25)-C(26)	1.413(5)	C(25)-H(25)	0.9500
C(28)-C(27)	1.412(4)	C(28)-H(28)	0.9500
C(26)-C(27)	1.421(5)	C(26)-H(26)	0.9500
C(27)-C(30)	1.548(5)	C(30)-H(30A)	0.9900
C(30)-H(30B)	0.9900	C(31)-C(39)	1.546(5)
C(31)-C(32)	1.547(5)	C(32)-C(33)	1.544(5)
C(32)-H(32A)	0.9900	C(32)-H(32B)	0.9900
C(33)-C(38)	1.410(5)	C(33)-C(34)	1.423(5)
C(34)-C(35)	1.412(5)	C(34)-H(34)	0.9500
C(35)-C(36)	1.425(4)	C(35)-H(35)	0.9500

C(36)-C(37)	1.419(5)	C(36)-C(36)#1	1.511(6)
C(37)-C(38)	1.410(5)	C(37)-H(37)	0.9500
C(38)-H(38)	0.9500	C(39)-C(40)	1.546(5)
C(39)-H(39A)	0.9900	C(39)-H(39B)	0.9900
C(40)-C(45)	1.414(5)	C(40)-C(41)	1.416(5)
C(41)-C(42)	1.408(4)	C(41)-H(41)	0.9500
C(42)-C(43)	1.426(5)	C(42)-H(42)	0.9500
C(43)-C(44)	1.420(5)	C(43)-C(43)#1	1.515(6)
C(44)-C(45)	1.414(5)	C(44)-H(44)	0.9500
C(45)-H(45)	0.9500		

O(1)-C(1)-C(30)	120.4(3)	O(1)-C(1)-C(2)	120.6(3)
C(30)-C(1)-C(2)	119.0(3)	C(1)-C(2)-C(3)	110.9(3)
C(1)-C(2)-H(2A)	109.5	C(3)-C(2)-H(2A)	109.5
C(1)-C(2)-H(2B)	109.5	C(3)-C(2)-H(2B)	109.5
H(2A)-C(2)-H(2B)	108.1	C(4)-C(3)-C(8)	117.9(3)
C(4)-C(3)-C(2)	122.0(3)	C(8)-C(3)-C(2)	119.8(3)
C(3)-C(4)-C(5)	121.0(3)	C(3)-C(4)-H(4)	119.5
C(5)-C(4)-H(4)	119.5	C(4)-C(5)-C(6)	121.3(3)
C(4)-C(5)-H(5)	119.3	C(6)-C(5)-H(5)	119.3
C(5)-C(6)-C(7)	117.3(3)	C(5)-C(6)-C(9)	122.6(3)
C(7)-C(6)-C(9)	119.9(3)	C(8)-C(7)-C(6)	121.1(3)
C(8)-C(7)-H(7)	119.5	C(6)-C(7)-H(7)	119.5
C(7)-C(8)-C(3)	121.2(3)	C(7)-C(8)-H(8)	119.4
C(3)-C(8)-H(8)	119.4	C(14)-C(9)-C(10)	117.1(3)
C(14)-C(9)-C(6)	121.7(3)	C(10)-C(9)-C(6)	121.1(3)
C(11)-C(10)-C(9)	121.1(3)	C(11)-C(10)-H(10)	119.5
C(9)-C(10)-H(10)	119.5	C(10)-C(11)-C(12)	121.6(3)
C(10)-C(11)-H(11)	119.2	C(12)-C(11)-H(11)	119.2
C(13)-C(12)-C(11)	117.6(3)	C(13)-C(12)-C(15)	120.0(3)
C(11)-C(12)-C(15)	122.4(3)	C(12)-C(13)-C(14)	121.1(3)
C(12)-C(13)-H(13)	119.5	C(14)-C(13)-H(13)	119.5
C(13)-C(14)-C(9)	121.4(3)	C(13)-C(14)-H(14)	119.3
C(9)-C(14)-H(14)	119.3	C(16)-C(15)-C(12)	115.3(3)
C(16)-C(15)-H(15A)	108.5	C(12)-C(15)-H(15A)	108.5
C(16)-C(15)-H(15B)	108.5	C(12)-C(15)-H(15B)	108.5
H(15A)-C(15)-H(15B)	107.5	O(2)-C(16)-C(17)	120.6(3)
O(2)-C(16)-C(15)	120.4(3)	C(17)-C(16)-C(15)	119.1(3)

C(16)-C(17)-C(18)	111.0(3)	C(16)-C(17)-H(17A)	109.4
C(18)-C(17)-H(17A)	109.4	C(16)-C(17)-H(17B)	109.4
C(18)-C(17)-H(17B)	109.4	H(17A)-C(17)-H(17B)	108.0
C(19)-C(18)-C(23)	117.8(3)	C(19)-C(18)-C(17)	121.2(3)
C(23)-C(18)-C(17)	120.8(3)	C(18)-C(19)-C(20)	121.3(3)
C(18)-C(19)-H(19)	119.3	C(20)-C(19)-H(19)	119.3
C(19)-C(20)-C(21)	121.0(3)	C(19)-C(20)-H(20)	119.5
C(21)-C(20)-H(20)	119.5	C(20)-C(21)-C(22)	117.7(3)
C(20)-C(21)-C(24)	120.8(3)	C(22)-C(21)-C(24)	121.3(3)
C(23)-C(22)-C(21)	121.0(3)	C(23)-C(22)-H(22)	119.5
C(21)-C(22)-H(22)	119.5	C(22)-C(23)-C(18)	121.1(3)
C(22)-C(23)-H(23)	119.4	C(18)-C(23)-H(23)	119.4
C(29)-C(24)-C(25)	117.7(3)	C(29)-C(24)-C(21)	120.1(3)
C(25)-C(24)-C(21)	122.0(3)	C(28)-C(29)-C(24)	121.1(3)
C(28)-C(29)-H(29)	119.5	C(24)-C(29)-H(29)	119.5
C(26)-C(25)-C(24)	120.8(3)	C(26)-C(25)-H(25)	119.6
C(24)-C(25)-H(25)	119.6	C(27)-C(28)-C(29)	121.5(3)
C(27)-C(28)-H(28)	119.2	C(29)-C(28)-H(28)	119.2
C(25)-C(26)-C(27)	121.4(3)	C(25)-C(26)-H(26)	119.3
C(27)-C(26)-H(26)	119.3	C(28)-C(27)-C(26)	117.4(3)
C(28)-C(27)-C(30)	121.0(3)	C(26)-C(27)-C(30)	121.5(3)
C(1)-C(30)-C(27)	112.0(3)	C(1)-C(30)-H(30A)	109.2
C(27)-C(30)-H(30A)	109.2	C(1)-C(30)-H(30B)	109.2
C(27)-C(30)-H(30B)	109.2	H(30A)-C(30)-H(30B)	107.9
O(3)-C(31)-C(39)	120.7(3)	O(3)-C(31)-C(32)	120.7(3)
C(39)-C(31)-C(32)	118.6(3)	C(33)-C(32)-C(31)	113.1(3)
C(33)-C(32)-H(32A)	109.0	C(31)-C(32)-H(32A)	109.0
C(33)-C(32)-H(32B)	109.0	C(31)-C(32)-H(32B)	109.0
H(32A)-C(32)-H(32B)	107.8	C(38)-C(33)-C(34)	118.1(3)
C(38)-C(33)-C(32)	120.8(3)	C(34)-C(33)-C(32)	121.1(3)
C(35)-C(34)-C(33)	121.0(3)	C(35)-C(34)-H(34)	119.5
C(33)-C(34)-H(34)	119.5	C(34)-C(35)-C(36)	120.7(3)
C(34)-C(35)-H(35)	119.6	C(36)-C(35)-H(35)	119.6
C(37)-C(36)-C(35)	117.7(3)	C(37)-C(36)-C(36)#1	120.2(4)
C(35)-C(36)-C(36)#1	121.7(4)	C(38)-C(37)-C(36)	121.2(3)
C(38)-C(37)-H(37)	119.4	C(36)-C(37)-H(37)	119.4
C(37)-C(38)-C(33)	121.1(3)	C(37)-C(38)-H(38)	119.5
C(33)-C(38)-H(38)	119.5	C(31)-C(39)-C(40)	112.4(3)

C(31)-C(39)-H(39A)	109.1	C(40)-C(39)-H(39A)	109.1
C(31)-C(39)-H(39B)	109.1	C(40)-C(39)-H(39B)	109.1
H(39A)-C(39)-H(39B)	107.9	C(45)-C(40)-C(41)	118.5(3)
C(45)-C(40)-C(39)	121.0(3)	C(41)-C(40)-C(39)	120.5(3)
C(42)-C(41)-C(40)	121.3(3)	C(42)-C(41)-H(41)	119.4
C(40)-C(41)-H(41)	119.4	C(41)-C(42)-C(43)	120.5(3)
C(41)-C(42)-H(42)	119.8	C(43)-C(42)-H(42)	119.8
C(44)-C(43)-C(42)	118.0(3)	C(44)-C(43)-C(43)#1	122.1(4)
C(42)-C(43)-C(43)#1	119.8(4)	C(45)-C(44)-C(43)	121.2(3)
C(45)-C(44)-H(44)	119.4	C(43)-C(44)-H(44)	119.4
C(40)-C(45)-C(44)	120.5(3)	C(40)-C(45)-H(45)	119.8
C(44)-C(45)-H(45)	119.8		

Symmetry transformations used to generate equivalent atoms:

#1 -x+1,y,-z+3/2

Table S5. Anisotropic displacement parameters (Å^2).

The anisotropic displacement factor exponent takes the form:

$-2\pi^2[\, h^2 a^{*2} U_{11} + ... + 2\, h\, k\, a^*\, b^*\, U_{12}\,]$.

	U_{11}	U_{22}	U_{33}	U_{23}	U_{13}	U_{12}
C(1)	0.019(2)	0.034(2)	0.019(2)	0.001(2)	0.009(1)	0.000(1)
C(2)	0.032(2)	0.028(2)	0.022(2)	0.002(2)	0.009(2)	-0.001(2)
O(2)	0.071(2)	0.048(2)	0.020(2)	0.000(1)	0.001(1)	0.003(2)
C(3)	0.034(2)	0.019(2)	0.020(2)	0.002(2)	0.009(2)	0.001(1)
O(3)	0.075(2)	0.051(2)	0.023(2)	0.005(2)	0.013(2)	0.011(2)
C(4)	0.027(2)	0.021(2)	0.024(2)	0.000(2)	0.003(2)	-0.003(1)
C(5)	0.036(2)	0.016(2)	0.018(2)	-0.002(2)	0.002(2)	0.000(1)
C(6)	0.033(2)	0.015(2)	0.016(2)	0.001(2)	0.006(2)	0.004(1)
C(7)	0.026(2)	0.031(2)	0.023(2)	-0.001(2)	0.003(2)	0.001(2)
C(8)	0.034(2)	0.031(2)	0.017(2)	-0.001(2)	0.005(2)	0.000(2)
C(9)	0.031(2)	0.018(2)	0.016(2)	-0.004(2)	0.005(2)	0.001(1)
C(10)	0.026(2)	0.025(2)	0.023(2)	-0.001(2)	0.002(2)	0.000(1)
C(11)	0.037(2)	0.025(2)	0.015(2)	0.000(2)	0.004(2)	0.000(2)
C(12)	0.033(2)	0.022(2)	0.019(2)	-0.003(2)	0.008(2)	0.001(2)
C(13)	0.028(2)	0.030(2)	0.027(2)	0.000(2)	0.006(2)	0.008(2)
C(14)	0.037(2)	0.024(2)	0.018(2)	0.002(2)	0.004(2)	0.007(2)
C(15)	0.035(2)	0.032(2)	0.032(2)	-0.003(2)	0.015(2)	0.003(2)
C(16)	0.024(2)	0.033(2)	0.024(2)	-0.002(2)	0.011(2)	0.001(2)
C(17)	0.033(2)	0.032(2)	0.032(2)	-0.004(2)	0.012(2)	-0.005(2)
C(18)	0.030(2)	0.026(2)	0.025(2)	-0.009(2)	0.010(2)	-0.006(2)
C(19)	0.026(2)	0.037(2)	0.027(2)	-0.008(2)	0.002(2)	-0.001(2)
C(20)	0.035(2)	0.030(2)	0.019(2)	-0.003(2)	0.002(2)	-0.002(2)
C(21)	0.030(2)	0.016(2)	0.019(2)	-0.004(2)	0.007(2)	-0.002(1)
C(22)	0.032(2)	0.020(2)	0.023(2)	0.001(2)	0.006(2)	0.004(1)
C(23)	0.041(2)	0.021(2)	0.022(2)	0.001(2)	0.011(2)	0.000(2)
C(24)	0.030(2)	0.015(2)	0.017(2)	0.002(2)	0.006(2)	0.002(1)
C(29)	0.035(2)	0.021(2)	0.017(2)	0.000(2)	0.002(2)	0.004(2)
C(25)	0.028(2)	0.023(2)	0.020(2)	-0.004(2)	0.003(2)	-0.003(1)
C(28)	0.026(2)	0.025(2)	0.024(2)	0.002(2)	0.000(2)	-0.001(1)
C(26)	0.036(2)	0.025(2)	0.016(2)	-0.001(2)	0.005(2)	0.002(2)
C(27)	0.030(2)	0.021(2)	0.021(2)	0.005(2)	0.007(2)	0.004(1)
C(30)	0.028(2)	0.029(2)	0.027(2)	0.003(2)	0.009(2)	0.002(2)

C(31)	0.027(2)	0.035(2)	0.022(2)	0.000(2)	0.000(2)	0.004(2)
C(32)	0.034(2)	0.026(2)	0.031(2)	0.001(2)	0.003(2)	0.006(2)
C(33)	0.030(2)	0.022(2)	0.024(2)	-0.002(2)	0.004(2)	0.006(1)
C(34)	0.043(2)	0.021(2)	0.017(2)	0.002(2)	0.005(2)	0.003(2)
C(35)	0.032(2)	0.018(2)	0.027(2)	0.000(2)	0.012(2)	-0.003(1)
C(36)	0.032(2)	0.015(2)	0.021(2)	-0.002(2)	0.007(2)	0.003(1)
C(37)	0.032(2)	0.028(2)	0.019(2)	0.001(2)	0.007(2)	0.004(2)
C(38)	0.026(2)	0.031(2)	0.031(2)	0.000(2)	0.014(2)	0.002(2)
C(39)	0.039(2)	0.027(2)	0.030(2)	-0.003(2)	-0.001(2)	0.000(2)
C(40)	0.037(2)	0.019(2)	0.021(2)	-0.003(2)	0.001(2)	0.002(2)
C(41)	0.038(2)	0.026(2)	0.016(2)	-0.001(2)	0.006(2)	0.002(2)
C(42)	0.030(2)	0.026(2)	0.023(2)	-0.002(2)	0.008(2)	0.000(2)
C(43)	0.035(2)	0.015(2)	0.018(2)	-0.002(2)	0.005(2)	0.002(1)
C(44)	0.037(2)	0.021(2)	0.024(2)	0.002(2)	0.009(2)	-0.002(2)
C(45)	0.029(2)	0.025(2)	0.029(2)	-0.001(2)	0.007(2)	-0.002(2)
O(1)	0.039(1)	0.045(2)	0.018(2)	-0.002(1)	0.002(1)	-0.001(1)

Table S6. Hydrogen coordinates and isotropic displacement parameters (Å^2).

	x	y	z	U_{eq}
H(2A)	0.4515	0.1507	0.2755	0.032
H(2B)	0.4843	0.1159	0.3520	0.032
H(4)	0.4598	0.1547	0.4936	0.029
H(5)	0.4062	0.1574	0.5938	0.028
H(7)	0.3143	0.1052	0.4023	0.032
H(8)	0.3682	0.0999	0.3032	0.033
H(10)	0.3577	0.0675	0.6753	0.029
H(11)	0.3027	0.0390	0.7686	0.031
H(13)	0.2136	0.1424	0.5913	0.034
H(14)	0.2685	0.1728	0.4976	0.032
H(15A)	0.2141	0.1050	0.7932	0.039
H(15B)	0.1869	0.0623	0.7123	0.039
H(17A)	0.1798	-0.1240	0.6959	0.038
H(17B)	0.2042	-0.1921	0.7658	0.038
H(19)	0.2124	-0.0988	0.5591	0.036
H(20)	0.2708	-0.1057	0.4704	0.033
H(22)	0.3461	-0.2206	0.6671	0.030
H(23)	0.2876	-0.2130	0.7554	0.034
H(29)	0.3974	-0.1087	0.6045	0.030
H(25)	0.3262	-0.1924	0.3898	0.028
H(28)	0.4563	-0.0772	0.5215	0.030
H(26)	0.3858	-0.1636	0.3077	0.031
H(30A)	0.4903	-0.0658	0.3878	0.034
H(30B)	0.4737	-0.1413	0.3158	0.034
H(32A)	0.3589	0.6468	0.5093	0.036
H(32B)	0.3428	0.5687	0.5756	0.036
H(34)	0.4454	0.6734	0.5179	0.032
H(35)	0.5062	0.6976	0.6116	0.031
H(37)	0.4384	0.5972	0.8095	0.031
H(38)	0.3785	0.5698	0.7150	0.035
H(39A)	0.3824	0.3566	0.4648	0.038
H(39B)	0.3505	0.3863	0.5370	0.038
H(41)	0.4654	0.4214	0.5103	0.032

H(42)	0.5207	0.4064	0.6178	0.031
H(44)	0.4319	0.3205	0.7857	0.033
H(45)	0.3768	0.3350	0.6772	0.033

Figure S10. The needle-like crystal of **MC**

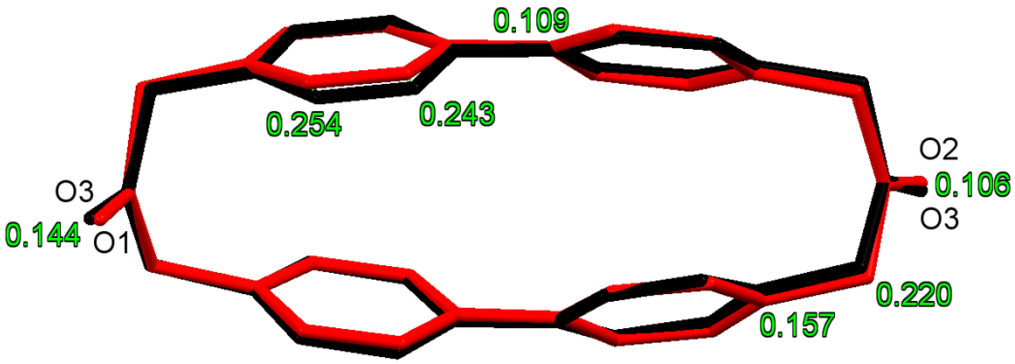

Figure S11. Superposition of the two independent molecules of **MC** in the crystal. Selected deviations are given in Å.

CCDC 1050402 contains the supplementary crystallographic data for **MC**. These data can be obtained free of charge via http://www.ccdc.cam.ac.uk/conts/retrieving.html, or from the Cambridge Crystallographic Data Centre, CCDC, 12 Union Road, Cambridge CB2 1EZ, UK (Fax: +44-1223-336-033; or E-Mail: deposit@ccdc.cam.ac.uk). We acknowledge the Synchrotron Light Source ANKA (KIT, Karlsruhe) for provision of instruments at their beamlines and thank *Dr. Gernot Buth* for his support at the SCD beamline.